Letters on Materials 15 (4), 2025 pp. 423-430 www.lettersonmaterials.com

Received 14 November 2025; Accepted 27 November 2025 https://elibrary.ru/odsbim
https://doi.org/10.48612/letters/2025-4-423-430

Microstructural development in the modeling and commercial Al-Cu based alloys during equal-channel angular pressing at elevated temperature
Part I. Microstructural evolution and continuous dynamic recrystallization in a model Al-3%Cu alloy

O. Sh. Sitdikov

sitdikov.oleg@imsp.ru

Institute for Metals Superplasticity Problems, Russian Academy of Sciences, Ufa 450001, Russia

Abstract: This study (Part I) investigates the microstructural evolution in a model Al-3%Cu alloy during equal-channel angular pressing at an elevated temperature of 300°C ($0.6T_m$). The use of a binary model alloy aims to isolate the fundamental grain refinement mechanisms without the confounding effects of transition metal dispersoids. Through scanning electron microscopy with electron backscatter diffraction and X-ray diffraction analysis, it is demonstrated that grain refinement occurs via continuous dynamic recrystallization. This process is primarily driven by the formation of permanent structural elements — microshear bands. The boundaries of these bands accumulate dislocations over successive equal-channel angular pressing passes, leading to a progressive increase in misorientation and their eventual transformation into high-angle grain boundaries. The θ-phase (Al_2Cu) precipitates play a critical dual role: they stabilize the deformation-induced structures by pinning dislocations and exerting Zener drag on boundaries, while simultaneously controlling local dislocation rearrangement that aids the formation of more equilibrium subgrain structures. Despite intense dynamic recovery and competing static softening processes during inter-pass annealing, dynamic refinement remains dominant. This work establishes microshear band-driven continuous dynamic recrystallization as a fundamental grain refinement mechanism in simple Al-Cu alloys, providing a crucial baseline for understanding the enhanced refinement in commercial alloys containing dispersoids, as will be reported in Part II.

Keywords: Al-3%Cu alloy, equal channel angular pressing, high temperature, microstructural evolution, grain refinement, continuous dynamic recrystallization, microshear bands, precipitates

Acknowledgements: *The research was supported by the Ministry of Science and Higher Education of the Russian Federation within the framework of the state assignment of IMSP RAS. The author is grateful to Prof. T. Sakai (UEC Tokyo, Japan) for fruitful discussions that contributed to this study. Some experimental results were obtained in the joint research with I. A. Mazurina and I. S. Oleneva.*

1. Introduction

Equal-channel angular pressing (ECAP) is a prominent severe plastic deformation (SPD) technique extensively used for producing bulk ultrafine-grained (UFG) materials [1–6]. The exceptional properties of UFG materials, such as high strength and potential for superplasticity, are well-documented [2,3]. The microstructural evolution during ECAP at low to moderate temperatures, which is primarily governed by the formation of a dislocation substructure and its transformation into high-angle grain boundaries, has been thoroughly studied in various alloys [3–6].

In contrast, the behavior of alloys during SPD at elevated temperatures (typically above $0.5T_m$) remains less explored [7–11]. At these temperatures, thermally activated processes like dynamic recovery and dynamic recrystallization become dominant, critically influencing the final microstructure [12]. While extensive dynamic recovery can impede the accumulation of dislocations necessary for grain refinement, it can also control the formation of the substructure, which is a precursor to continuous dynamic recrystallization (cDRX) [11–13].

A significant body of research on high-temperature SPD has focused on complex commercial alloys containing transition metals (e.g., Zr, Mn, Cr, Sc) [14]. These elements form nanoscale dispersoids that enhance the thermal stability of the microstructure [3,8,11,14–17]. However, the presence of these stable particles can obscure the fundamental mechanisms of grain refinement and misorientation evolution, making it difficult to extrapolate these findings to simpler alloy systems. To decouple the intrinsic effects of SPD from the additional influence of dispersoids, studies on model alloys not containing transition metals are essential.

This study, presented in two parts, aims to provide a comprehensive understanding of microstructural development during high-temperature ECAP of Al-Cu alloys. In the first part, a model Al-3%Cu alloy is employed to isolate the fundamental mechanisms of grain refinement. The primary objectives of this work are:

(i) to elucidate the microstructural evolution and the mechanism of grain refinement in a model binary Al-Cu alloy during ECAP at 300°C (0.6T_m);

(ii) to quantitatively characterize the development of deformation-induced boundaries, caused by a strain heterogeneity with a particular focus on the role of deformation/shear bands, as permanent structural elements, driving the refinement process [5,6,18–20];

(iii) to analyze the competition between dynamic grain refinement and concomitant static softening processes that occur during inter-pass annealing [9,21].

The use of a binary model alloy allows us to clarify the role of basic second-phase θ (Al_2Cu) precipitates, without the complicating effects of fine dispersoids, thereby establishing a baseline understanding of cDRX in Al-Cu alloys under high-temperature SPD conditions.

2. Materials and methods

An ingot of the model alloy Al-3 wt.% Cu was homogenized at 520°C for 4 hours, followed by furnace cooling to eliminate dendritic segregation and promote the formation of equilibrium precipitates of the θ-phase (Al_2Cu).

Cylindrical samples, measuring 20 mm in diameter and 100 mm in length, were machined from the homogenized ingot. Isothermal ECAP was performed at 300°C using a hydraulic press and a die with channel intersection angles of $\Phi = 90°$ and $\Psi = 0°$. This configuration imposes an equivalent strain of approximately $\Delta e \approx 1$ per pass [4–6]. Processing was conducted following route A (no sample rotation between passes) for up to 12 passes, resulting in a total accumulated strain of $e \approx 12$. The pressing speed was maintained at 6 mm/s, resulting in an approximate strain rate of 3 s^{-1}. To preserve the deformation structure, the samples were water-quenched immediately after each pass. Before the next operation, they were reheated to 300°C and held for 45 minutes to provide consistent inter-pass conditions.

Microstructural analysis was carried out on longitudinal sections parallel to the pressing direction (PD). For optical microscopy, mechanically polished samples were etched with Keller's reagent. Specimens for electron microscopy were prepared by electropolishing in a solution of 30% HNO_3 and 70% CH_3OH at 20 V and −30°C. Scanning electron microscopy (SEM) coupled with electron backscatter diffraction (EBSD) was performed using TESCAN MIRA 3 LMH and LEO-1530 field-emission microscopes, both equipped with HKL Channel 5 software. The microscopes were operated at 20 kV with a beam current of ≈2.2 nA. The scan step size was set between 0.1 and 0.4 μm to ensure an average of at least five measurement points per crystallite. Standard noise reduction procedures were applied to eliminate non-indexed points.

For the analysis of EBSD data, inverse pole figure (IPF) maps were used. Boundaries between measurement points were classified and visualized as follows: low-angle boundaries (LABs, $2° \leq \theta < 5°$) as thin white lines, medium-angle boundaries (MABs, $5° \leq \theta < 15°$) as thin dark gray lines, and high-angle boundaries (HABs, $\theta \geq 15°$) as bold black lines. For the "deformed – subgrained – recrystallized" component maps, areas with high lattice distortion (>2°) bounded by HABs were colored dark, subgrained areas (containing LABs/MABs) were colored gray, and recrystallized areas were colored white. Boundaries with misorientation below 2° were excluded from the analysis. The grain size was determined using the equivalent circle diameter method. The volume fraction of new fine grains was calculated using the point counting technique. X-ray diffraction analysis was performed on a 1 mm diameter area using the photograph method with a URS 2.0 device to qualitatively assess structure and texture development and lattice strain.

3. Results

3.1. Precipitate features in the model Al-3%Cu alloy

Homogenization treatment of the model Al-3%Cu alloy produced a uniform, equiaxed α-Al solid solution matrix with grain sizes ranging from 100 to 400 μm [9,10]. The structure was characterized by the presence of numerous secondary θ (Al_2Cu) phase precipitates, which formed during slow cooling of the ingot to room temperature (Fig. 1a). These θ-phase precipitates were distributed both heterogeneously at grain boundaries and homogeneously within the grains [10]. Consequently, this treatment resulted in a non-uniform distribution of precipitates with sizes ranging from approximately 0.01 to 3 μm.

Subsequent heating and a one-hour hold at 300°C, simulating the pre-heating stage for isothermal ECAP, led to partial dissolution and coarsening/spheroidization of the secondary phases (Fig. 1b). However, the overall distribution pattern was maintained, and the precipitate sizes remained within the previously mentioned range. After this treatment, the microstructure contained predominantly Al_2Cu precipitates, which acted as the main strengthening phase in the model alloy. According to the phase diagram, the equilibrium volume fraction of the Θ-phase, calculated using the lever rule, is approximately 5.6% at room temperature and 5.2% at 300°C [9].

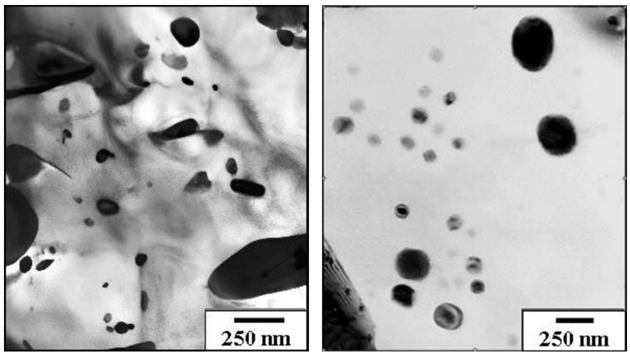

a b

Fig. 1. Typical TEM images of second-phase precipitates in the model Al-3%Cu alloy: after homogenization (a); after homogenization and subsequent quenching from 300°C (b).

3.2. Microstructural evolution in the model Al-3%Cu alloy

The microstructural development in the Al-3%Cu alloy during ECAP at 300°C exhibited a marked strain dependence, characterized by the formation and evolution of pronounced strain localization phenomena. After the initial passes (to a strain of $e \approx 1-4$), the initial equiaxed grain structure transformed into a microstructure of grains elongated and progressively aligned with the PD, as revealed by optical microscopy (Fig. 2a–c).

Within these grains, significant local lattice rotations and distortions were observed, with misorientations sometimes exceeding 2° per 1–2 μm (Fig. 3a, b). These distortion angles are indicative of the high dislocation density (typically on the order of 10^{13} to 10^{14} m^{-2}) introduced by SPD [17]. Concurrently, heterogeneous deformation bands developed as an early manifestation of strain localization. These bands, with lengths exceeding 400 μm and widths varying between 6 and 40 μm, became a defining feature of the microstructure.

EBSD analysis (IPF map) of the sample deformed to $e=1$ (Fig. 4a) showed that in some grains, these bands were delineated by segments of MABs and HABs. The pole figures corresponding to points a–d in Fig. 4b illustrate a significant crystallographic reorientation inside the bands compared to the surrounding matrix. The matrix orientation remained relatively stable, while the lattice within the bands underwent a pronounced rotation of approximately 10–15°, resulting in a new orientation common to all bands.

This misorientation evolution was quantified along an arbitrary transect, T_1, in Fig. 5a. The profile showed a sharp increase in both point-to-point ($\Delta\theta$) and cumulative point-to-origin ($\Sigma\Delta\theta$) misorientation, reaching up to 15° over a distance of less than 10 μm. These findings confirm the role of such features as precursors to new high-angle boundaries. The characteristic step-like misorientation profiles with alternating cumulative misorientations are typical of microshear bands, which are frequently reported in aluminum alloys subjected to SPD [6,8,10,11,18,19]. Additional strain heterogeneity was revealed by the formation of new orientations near original grain boundaries (point e, Fig. 4a).

In contrast, other grains exhibited a more uniform deformation structure composed primarily of LABs, with only isolated MABs (e.g., points f and g, Fig. 4a). The misorientation profile along line T_2 (Fig. 5b) for such regions showed frequent, small fluctuations in both $\Delta\theta$ and $\Sigma\Delta\theta$, which is characteristic of a developing, dynamically equilibrated subgrain structure [7,8,10–13].

It is important to note that, unlike a dynamically equilibrated subgrain structure — which is incidental by

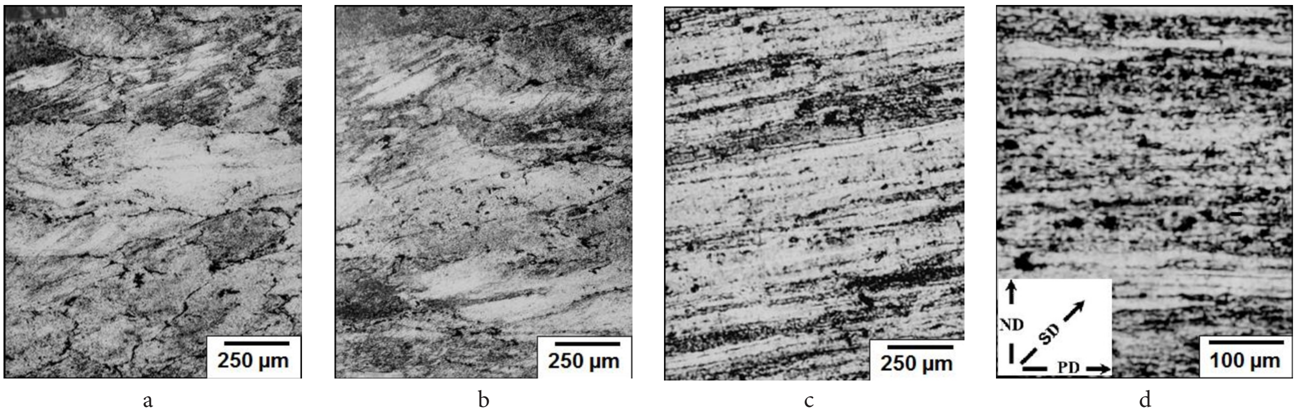

Fig. 2. Optical micrographs of the Al-3%Cu alloy after ECAP at 300°C to various strains: $e=1$ (a), $e=2$ (b), $e=4$ (c), $e=12$ (d). Hereafter, PD denotes the pressing direction; ND is the normal direction; SD is the main shear direction in ECAP.

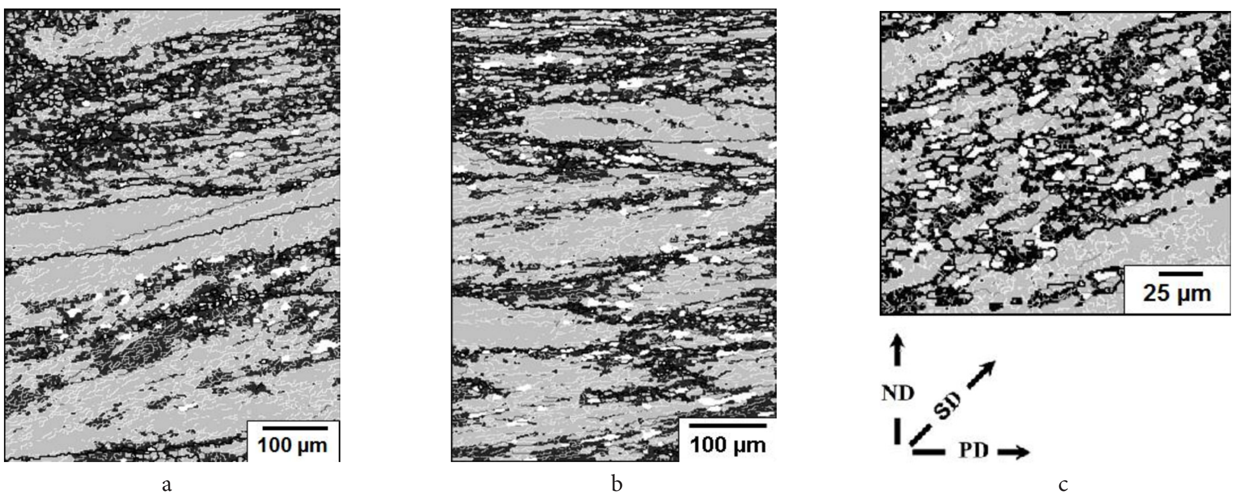

Fig. 3. Typical EBSD maps illustrating the deformation–subgrain–recrystallization microstructure developed in the Al-3%Cu alloy during ECAP at $T=300$°C to: $e=1$ (a), $e=2$ (b), $e=8$ (c).

nature (i. e., it can form and be destroyed at comparable rates during the steady state of plastic flow [11–13]) — microshear bands represent permanent structural elements [5,10,18–20]. Consequently, once formed, they persist and continue to accommodate strain during subsequent deformation passes.

With increasing strain ($e = 2-4$), the number and density of microshear bands increased significantly. The original grains, now containing these bands, became increasingly aligned along the PD, forming a microstructure of alternating fibers delineated by HABs and MABs (Fig. 2b, c). Concurrently, new microshear bands developed during each pass, aligning with the shear direction (SD) and intersecting the pre-existing deformed structure. This intersection led to the progressive fragmentation of the original grains.

At strains of $e = 4-8$, EBSD maps (Fig. 3c, 6a, b) revealed the emergence of new, finer crystallites, particularly in regions

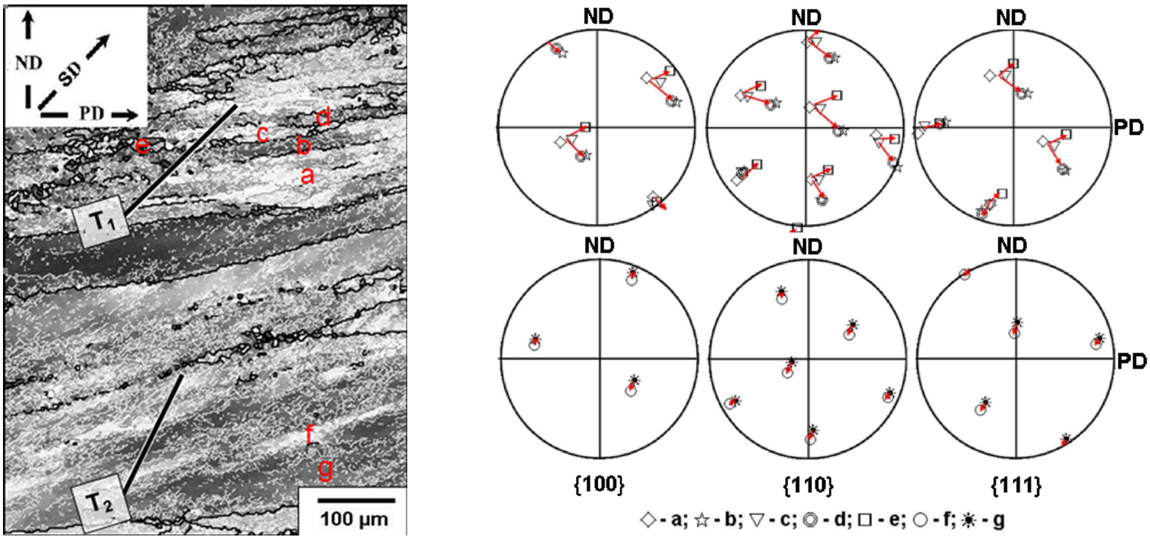

a b

Fig. 4. Microstructure of the Al-3%Cu alloy after ECAP at 300°C to $e = 1$: Inverse pole figure (IPF) map showing the distribution of grain and subgrain structures (a); Direct pole figures showing crystallographic orientations at points a through g marked in (a) (b).

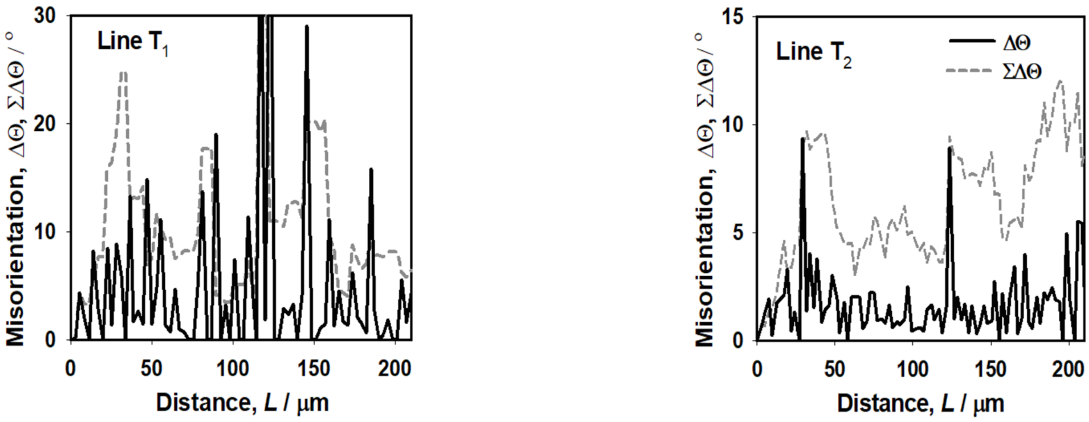

a b

Fig. 5. Point-to-point ($\Delta\theta$) and point-to-origin ($\Sigma\Delta\theta$) misorientation changes along the lines T_1 (a) and T_2 (b) indicated in Fig. 4.

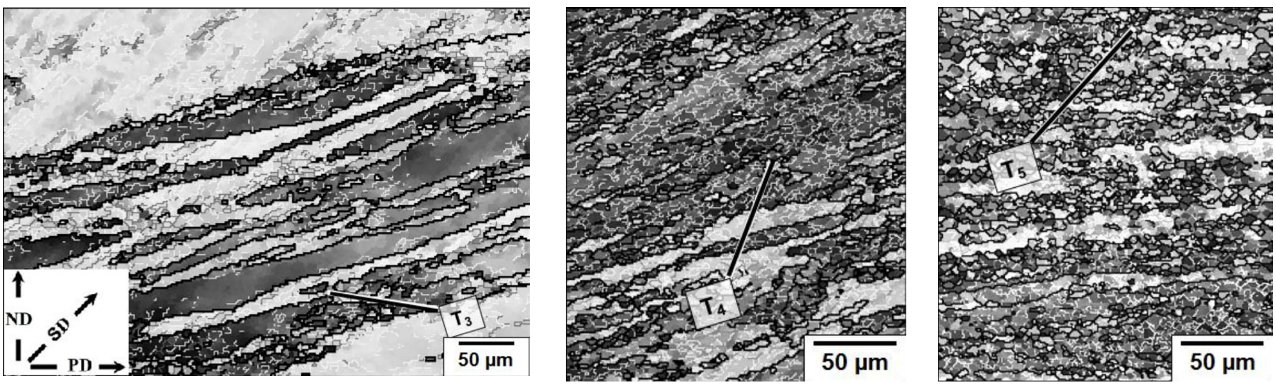

a b c

Fig. 6. Typical IPF-EBSD maps of the microstructure developed in the Al-3%Cu alloy during ECAP at 300°C to: $e = 4$ (a), $e = 8$ (b), $e = 12$ (c).

with a high density of band intersections. The formation of these crystallites was accompanied by an increase in the number and height of peaks in the misorientation profiles (Fig. 7a, b), measured along transects T_3 and T_4 in Fig. 6 a and b. Therewith, the misorientation $\Delta\theta$ reached values exceeding 15 – 20°. This suggests that the boundaries of the microshear bands underwent a continuous increase in misorientation, progressively transitioning from MABs to HABs.

After 12 passes ($e \approx 12$), a partially refined microstructure was observed (Fig. 2 d). Although remnants of the original deformed structure were still present, a fraction of new fine grains had formed throughout the material. The corresponding EBSD analysis (Fig. 6 c) revealed a final microstructure consisting of an UFG matrix with arrays of MABs and HABs, intersected by the measurement line T_5 (see Fig. 7c). The average crystallite size was as high as approximately 6.0 μm with the volume fraction of new grains of about 40–50%.

Figure 8 shows the misorientation distribution spectra (i. e., the relative fractions of LABs, MABs, and HABs) for the Al-3%Cu alloy after ECAP to different strains, along with the corresponding average misorientation angles (θ_{ave}) and HAB fractions (f_{HABs}). At low strains (e=1– 2), the misorientation distribution was typical for structures formed by low-temperature SPD of cubic metals [5,6,19]. The spectrum was dominated by LABs, with a significant population of strain-induced MABs. These MABs correspond to the deformation/microshear band boundaries described in the previous sections. With further straining to $e > 4$, the HAB fraction increased substantially, reaching approximately 45%. This increase is attributed primarily to the continuous transformation of MABs into HABs and the formation of new fine grains [12].

The X-ray diffraction patterns (Fig. 9 a – d) corroborate these findings. With increasing strain, the development of more continuous diffraction rings in the azimuthal direction, along with significant peak broadening, is consistent with the formation of a finer, more misoriented grain structure and the accumulation of lattice strains.

In summary, grain refinement in the Al-3%Cu alloy during high-temperature ECAP occurred via mechanisms akin to cDRX [8,10 –13,18]. This process involves the formation of a deformation substructure with LABs and MABs (e. g., microshear band boundaries) and its subsequent in-situ transformation into new grain boundaries, absent a significant grain growth stage. Crucially, this refinement pathway remained effective even under conditions of intense dynamic recovery, underscoring the robustness of the microshear banding mechanism.

As evidenced by the prevalence of dark and gray regions in the SEM-EBSD maps (Fig. 3), corresponding to areas of high lattice distortion and subgrain structures, the material retained a significant density of dislocations throughout the ECAP process. Thus, this accumulated stored strain energy provided the essential thermodynamic driving force for the formation of new grain boundaries via the cDRX mechanism.

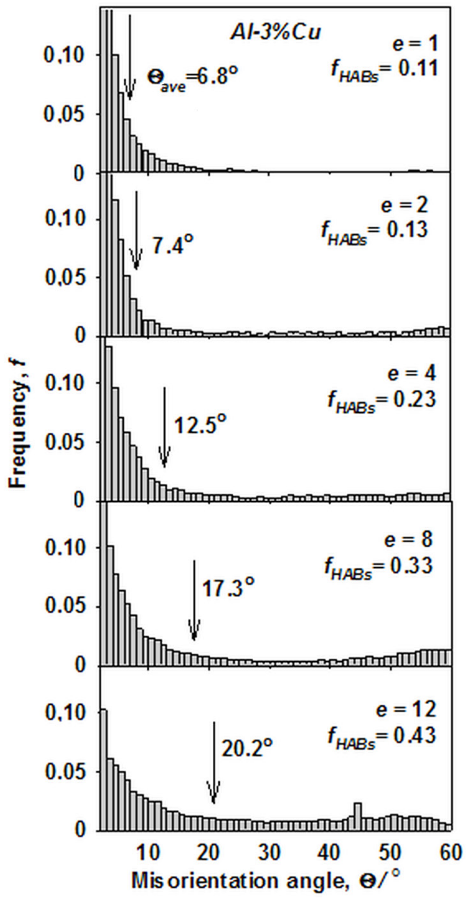

Fig. 8. Misorientation distributions of intercrystallite boundaries developed in the alloy Al-3%Cu during ECAP at $T = 300$°C.

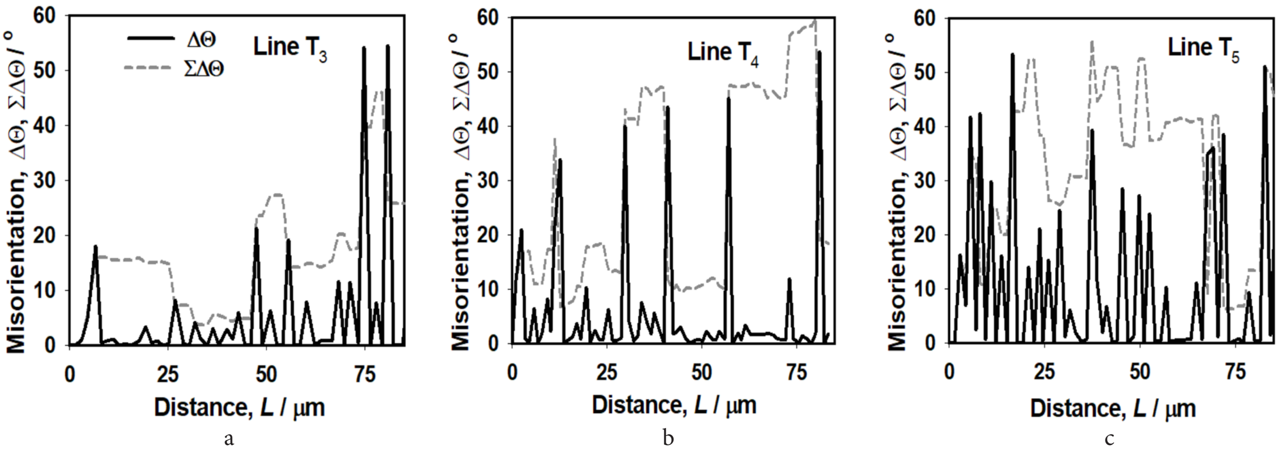

Fig. 7. The $\Delta\theta$ and $\Sigma\Delta\theta$ misorientation changes along the lines T_3 (a), T_4 (b) and T_5 (c) indicated in Fig. 6.

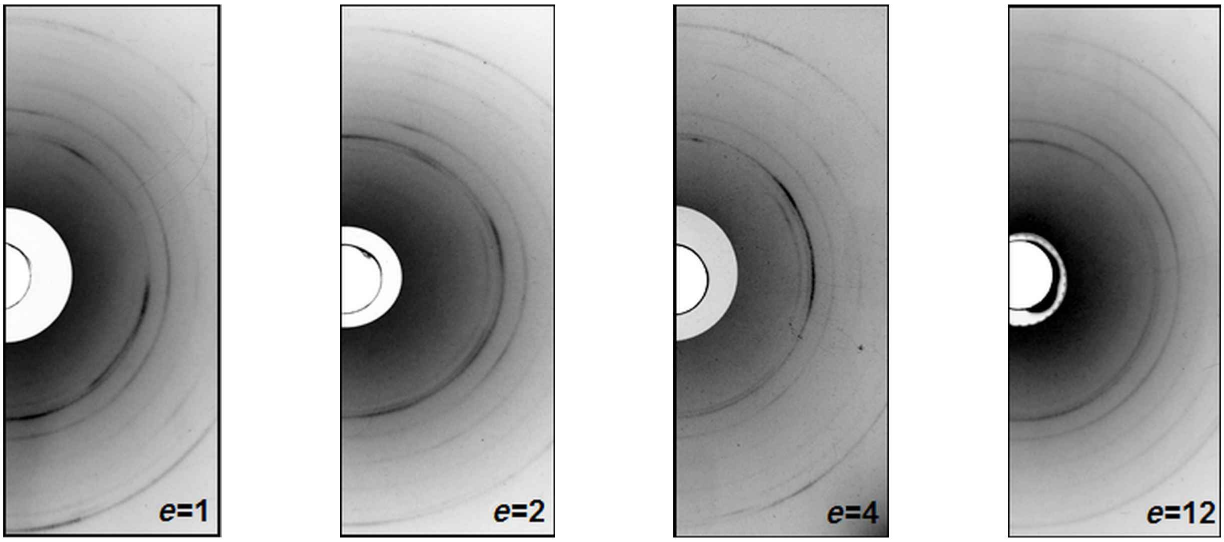

a b c d

Fig. 9. X-ray diffraction patterns of the alloy Al-3%Cu after ECAP at 300°C: $e=1$ (a), $e=2$ (b), $e=4$ (c) and $e=12$ (d).

However, the high processing temperature also enhanced the rates of static recovery and recrystallization [9, 21], which acted to reduce the stored energy. It is estimated that up to 90% of the total processing time was effectively a static anneal at high temperature [9]. This occurred for two reasons: first, the workpiece could not be cooled immediately after leaving the deformation zone, meaning it remained hot in the output channel; second, static processes occurred during the heating and holding stages prior to each subsequent pass.

Thus, at elevated temperature, static softening processes became highly competitive with dynamic ones. Nevertheless, as shown in Fig. 3, the fraction of statically recrystallized grains (featured by white areas) remained limited, not exceeding 10–15% even after $e=8$. One of key factors contributing to the accumulation of defects and the thermal stabilization of the microstructure was the presence of second-phase particles, which will be discussed in the following sections.

4. Discussion

4.1. Predominant grain refinement mechanism: cDRX via microshear banding

The present results, consistent with previous detailed studies on the same model alloy under similar warm ECAP conditions [10,15], demonstrate that the fundamental mechanism of grain refinement is cDRX. As mentioned above, this process is characterized by the *in-situ* transformation of deformation-induced boundaries into new high-angle boundaries without the growth stage typical of discontinuous recrystallization [12].

The key structural element driving cDRX in the Al-3%Cu alloy is the microshear band [10,11,18,19,22–24]. As shown in Sections 3.2, microshear bands act as permanent deformation features that accumulate strain over successive ECAP passes. Their boundaries, initially of low- to medium-angle character, undergo a continuous increase in misorientation due to the accumulation of dislocations, eventually transitioning into HABs that delineate new fine grains. This is evidenced by the progressive increase in both the average misorientation angle (θ_{ave}) and the HAB fraction (f_{HABs}) with strain (Fig. 8). A critical aspect of this mechanism is the intersection of microshear bands developed in different passes. The most significant lattice rotations occur precisely at these intersections, making them the predominant sites for the nucleation of new grains [10, 22, 23]. With further straining, new ultrafine grains form first at these intersections, followed by their development along the interiors of the bands.

4.2. The transition from cold to hot deformation structure

The processing temperature of 300°C ($0.6T_m$) in the present study is higher than the typical "warm" range (150°C, $\approx 0.5T_m$) described in [10]. This leads to an important observation regarding the competition between different types of deformation structures.

At 150°C, the early stages of ECAP are characterized by well-developed dislocation structures typical of "cold" deformation, such as cell blocks and microshear bands [5, 6,10, 20]. In this study at 300°C, the formation of a more homogeneous, dynamically equilibrated subgrain structure is more pronounced, which is characteristic of "hot" deformation [10,13, 22]. However, even under these conditions of enhanced dynamic recovery, the mechanism of microshear banding persists. This indicates that microshear banding is a robust, athermally activated mechanism [8] that can operate effectively even when competing against intense recovery processes. The final, partially refined microstructure observed in this study after 12 passes (≈6.0 μm) is coarser than the UFG structure achieved at 150°C after 8 passes (≈1.2 μm) [10], highlighting the limiting effect of higher temperature on the kinetics and efficiency of grain refinement.

4.3. The dual role of second-phase θ (Al_2Cu) precipitates

The θ-phase precipitates in the model alloy play a complex and dual role in the structure evolution, critically controlling the balance between grain refinement and recovery:

(i) stabilization of the deformation microstructure. The precipitates interact with dislocations and (sub)grain boundaries, pinning these defects and restricting long-range dislocation rearrangement/annihilation and boundary migration [10,14]. This pinning is crucial for stabilizing the deformation-induced boundaries of microshear bands against complete recovery, thereby allowing them to accumulate dislocations and progressively increase their misorientation towards high-angle boundaries. They provide essential dislocation pinning as well as a Zener drag force on intercrystallite interfaces, which retains the stored strain energy and enables the cDRX process to proceed.

(ii) control of structure transformation toward a more equilibrium state. It should be noted that the boundaries of deformation/microshear bands are initially rather non-equilibrium and diffuse interfaces [10,22]. Thus, the occurrence of dynamic recovery at a certain rate is required to release the internal stresses evolved by plastic working and promote dislocation rearrangement within the microshear bands, resulting in the formation of well-defined grain boundaries [22]. Simultaneously, the precipitates influence these recovery processes [14,22]. During ECAP at elevated temperature, the fine Al_2Cu precipitates coarsen (e.g., from ≈15 nm to ≈35 nm at 150°C [10]). This coarsening facilitates short-range dislocation rearrangement within cell/microshear band boundaries. While this reduces the overall stored energy, it also aids the transformation of diffuse dislocation boundaries into more equilibrium (sub)grain structures, which is a necessary step in the cDRX mechanism.

Thus, the θ-phase precipitates are essential participants in the microstructural evolution. Their role is based on a trade-off: they primarily stabilize the deformation structure to enable cumulative misorientation accumulation, while their secondary, coarsening-induced effect is to facilitate the local reorganization of dislocations, contributing to the formation of more defined grain boundaries. This dual role supports the cDRX process, even if it proceeds at a slower rate compared to the dispersion-strengthened alloy, as will be shown in Part II.

4.4. Competition between dynamic and static softening processes

The present ECAP processing at 300°C, which included inter-pass heating and holding, created conditions favorable for static recovery and recrystallization [9,21]. Despite these conditions, the fraction of statically recrystallized grains remained low (<15%, Fig. 3). This indicates that the θ-phase precipitation structure was effective in stabilizing the deformation microstructure [14] against static restoration processes during the inter-pass anneals.

The higher processing temperature in our study (300°C vs. 150°C in [10]) undoubtedly intensified this competition. Nevertheless, the dynamic refinement process dominated, underscoring the stability provided by the second-phase particles and the persistence of the microshear banding mechanism.

5. Conclusions

1. Grain refinement in the model Al-3%Cu alloy during ECAP at 300°C occurs via the mechanism of cDRX, primarily driven by the formation, intersection, and progressive increase in boundary misorientation of microshear bands.

2. The refinement kinetics at 300°C are slower, and the final microstructure is coarser (≈6.0 μm) compared to processing at lower temperatures (e.g., ≈1.2 μm at 150°C), due to the enhanced role of dynamic recovery.

3. The θ-phase (Al_2Cu) precipitates play a decisive dual role, enabling the cDRX process: they stabilize deformation-induced structures via dislocation pinning and Zener drag, while they simultaneously control short-range dislocation rearrangement, aiding the formation of a more equilibrium (sub)grain structure.

4. The presence of second-phase particles effectively stabilizes the deformation microstructure against static softening during inter-pass annealing, ensuring that dynamic refinement processes dominate.

5. The study establishes the microshear band-driven cDRX as a fundamental grain refinement mechanism in model Al-Cu alloys, providing a critical baseline for understanding the additional acceleration effects provided by dispersoids in commercial alloys (Part II).

References

1. R.Z. Valiev, R.K. Islamgaliev, I.V. Alexandrov, Bulk nanostructured materials from severe plastic deformation, Prog. Mater. Sci. 45 (2000) 103–189.
2. R.R. Mulyukov, R.M. Imayev, A.A. Nazarov, M.F. Imayev, V.M. Imayev, Superplasticity of ultrafine grained alloys: Experiment, theory, technologies, Nauka, Moscow, 2014. (in Russian)
3. K. Edalati, A. Bachmaier, V.A. Beloshenko, Y. Beygelzimer, V.D. Blank, W.J. Botta, K. Bryła, J. Čížek, S. Divinski, N.A. Enikeev, Y. Estrin, G. Faraji, R.B. Figueiredo, M. Fuji, T. Furuta, T. Grosdidier, J. Gubicza, A. Hohenwarter, Z. Horita, X. Zhu, Nanomaterials by severe plastic deformation: Review of historical developments and recent advances, Mater. Res. Lett. 10 (2022) 163–256.
4. R.Z. Valiev, T.G. Langdon, Principles of equal-channel angular pressing as a processing tool for grain refinement, Prog. Mater. Sci. 51 (2006) 881–981.
5. I.J. Beyerlein, L.S. Tóth, Texture evolution in equal-channel angular extrusion, Prog. Mater. Sci. 54 (2009) 427–510.
6. V. Segal, Review: Modes and Processes of Severe Plastic Deformation (SPD), Materials 11 (2018) 1175.
7. U. Chakkingal, P.F. Thomson, Development of microstructure and texture during high temperature equal channel angular extrusion of aluminium, J. Mater. Process. Technol. 117 (2001) 169–177.
8. I. Mazurina, T. Sakai, H. Miura, O. Sitdikov, R. Kaibyshev, Effect of deformation temperature on microstructure evolution in aluminum alloy 2219 during hot ECAP, Mater. Sci. Eng. A. 486 (2008) 662–671.
9. O.S. Sitdikov, E.V. Avtokratova, R.R. Zagitov, M.V. Markushev, Influence of the temperature of equal-channel angular pressing on fine-grain structure formation in the alloy Al-3% Cu, Lett. Mater. 11 (2021) 332–337.
10. O. Sitdikov, E. Avtokratova, M. Markushev, T. Sakai,

Structural characterization of binary Al-Cu alloy processed by equal channel angular pressing at half of the melting point, Metall. Mater. Trans. A 54 (2023) 505 – 525.
11. O.S. Sitdikov, Structural changes in a commercial Al-Cu alloy during hot equal channel angular pressing, Mater. Phys. Mech. 53 (2025) 89 –108.
12. F.J. Humphreys, M. Hatherly, Recrystallization and Related Annealing Phenomena, 2nd ed., Elsevier, Oxford, 2004, 628 p.
13. R. Zhang, J.S. Zhang, W. Wang, Y.T. Tang, J. Jiang, R.C. Reed, J. Lin, Mechanistic insights and kinetics of continuous and geometric dynamic recrystallisation in hot deformed aluminium alloy, Acta Mater. 289 (2025) 120893.
14. T.-S. Liu, B.-X. Dong, H.-Y. Yang, F. Qiu, S.-L. Shu, Q.-C. Jiang, Review on role of intermetallic and ceramic particles in recrystallization driving force and microstructure of wrought Al alloys, J. Mater. Res. Technol. 27 (2023) 3374 – 3395.
15. M.V. Markushev, O.S. Sitdikov, E.V. Avtokratova, Nanostructuring, structure heterogeneity, and static strength of complex aluminum alloys, Phys. Mesomech. 28 (2025) 381– 396.
16. A.G. Mochugovskiy, L.Y. Kaplanskaya, A.O. Mosleh, V.V. Palacheva, A.V. Mikhaylovskaya, Microstructure evolution and constitutive modelling of deformation behavior for Al-Mg-Si-Cu-Sc-Zr alloy processed with isothermal multidirectional forging, Appl. Sci. 13 (2023) 13054.
17. O.S. Sitdikov, E.V. Avtokratova, S.V. Krymskyi, R.R. Ilyasov, M.V. Markushev, Effect of severe forging and rolling on the microstructure and mechanical properties of Al-Mg-Sc-Zr alloy, Inorg. Mater. 57 (2021) 101–111.
18. O. Sitdikov, T. Sakai, A. Goloborodko, H. Miura, Grain fragmentation in a coarse-grained 7475 Al alloy during hot deformation, Scr. Mater. 51 (2004) 175 –179.
19. P.J. Apps, M. Berta, P.B. Prangnell, The effect of dispersoids on the grain refinement mechanisms during deformation of aluminium alloys to ultra-high strains, Acta Mater. 53 (2005) 499 – 511.
20. P.J. Hurley, F.J. Humphreys, The application of EBSD to the study of substructural development in a cold rolled single-phase aluminium alloy, Acta Mater. 51 (2003) 1087–1102.
21. O. Sitdikov, E.V. Avtokratova, R.I. Babicheva, T. Sakai, K. Tsuzaki, Y. Watanabe, Influence of processing regimes on fine-grained microstructure development in an Al-Mg-Sc alloy by hot equal-channel angular pressing, Mater. Trans. 53 (2012) 56 – 62.
22. O. Sitdikov, E. Avtokratova, T. Sakai, K. Tsuzaki, Ultrafine-Grain Structure Formation in an Al-Mg-Sc Alloy During Warm ECAP, Metall. Mater. Trans. A 44 (2013) 1087–1100.
23. O. Sitdikov, T. Sakai, H. Miura, C. Hama, Temperature effect on fine-grained structure formation in high-strength Al alloy 7475 during hot severe deformation, Mater. Sci. Eng. A 516 (2009) 180 –188.
24. K. Huang, R.E. Logé, A review of dynamic recrystallization phenomena in metallic materials, Mater. Des. 111 (2016) 548 – 574.